*Korean J. Chem. Eng.*, 37(2), 366-373 (2020)
DOI: 10.1007/s11814-019-0438-0

pISSN: 0256-1115
eISSN: 1975-7220

# Preparation of pectin-based dual-crosslinked network as a binder for high performance Si/C anode for LIBs

**Bolormaa Gendensuren, Chengxiang He, and Eun-Suok Oh†**

School of Chemical Engineering, University of Ulsan, 93 Daehak-ro, Nam-gu, Ulsan 44610, Korea
(*Received 16 September 2019 • accepted 21 November 2019*)

**Abstract**−The modification of pectin polysaccharide through grafting with polyacrylamide and crosslinking is newly proposed as a powerful candidate for a water-soluble binder of high-capacity Si anodes in lithium ion batteries. The grafting of pectin with polyacrylamide enhances adhesion in the electrode and contributes to the good wettability of the carbonate electrolyte. Herein, dual-crosslinking of pectin-*g*-polyacrylamide was achieved by the ionic crosslinking of pectin with divalent calcium ions and the chemical crosslinking of polyacrylamide with a bisacrylamide. As a result, the dual-crosslinked binder improves further the cycling performance of the Si/C composite anode with a 1.2 mg $cm^{-2}$ loading, which retains a specific capacity of 729 mAh $g^{-1}$ after 300 cycles. In contrast, the Si/C electrode containing dual-crosslinked alginate with polyacrylamide shows a specific capacity of 515 mAh $g^{-1}$ after 300 cycles.

Keywords: Polyacrylamide, Binder, Dual-crosslinked Polymer, Lithium-ion Battery, Silicon/Graphite High Capacity Electrode

## INTRODUCTION

The development of new electrode materials with high energy and power densities for lithium ion batteries (LIBs) has attracted considerable attention over the last 20 years [1-3]. A binder material, in particular, which provides integrity to composite electrodes consisting of active materials and conducting agents, has received increasing attention recently because it greatly influences the long-term cycling stability, rate capability, and irreversible capacity loss of the electrodes. The breakthrough for high capacity anodes experiencing large volume changes, such as silicon, depends strongly on the appropriate choice of polymeric binder. Polyvinylidene difluoride (PVdF) is the most common binder used in commercial LIBs. On the other hand, the Si electrode comprised of PVdF binder showed rapid capacity fading at less than twenty cycles because of its poor adhesion strength to the current collector [4,5]. Moreover, it dissolves only in toxic and expensive organic solvents, e.g., m-methyl-2-pyrrolidone, leading to environmental issues for the electrode manufacturing process.

To replace the organic solvent, environmentally friendly water soluble polymers, such as polyacrylic acid (PAA) [6], polyvinyl alcohol (PVA) [7], carboxymethyl cellulose (CMC) [8], and sodium alginate (Alg) [9-11], have been applied to high capacity Si-based anodes. They have shown excellent binder performance compared to the conventional PVdF binder, owing to their robust adhesion to the active material and current collector and low electrolyte swelling, which maintains the mechanical properties of the binder. Recently, the grafting and/or the crosslinked network in a binder composed of three water soluble polymers was reported to be more favorable in Si anodes. PAA-*g*-CMC, which is PAA grafted with CMC, enhanced the electrochemical performance for Si electrodes, having a high mass loading because of the good adhesion to current collector and the formation of a stable solid electrolyte interface (SEI) layer on the Si surface by the branched structure of PAA-*g*-CMC, compared to the sole use of a linear polymeric binder, PAA or CMC [12]. Zhang et al. [13] and Liu et al. [14] reported that the ionic crosslinking of Alg by divalent $Ca^{2+}$ ions improved the mechanical strength, recovery effect, and cycling stability of Si-based anodes. Kim et al. [15] developed a renatured DNA-Alg crosslinked binder for Si based anodes to facilitate homogeneous distribution of electrode materials due to the amphiphilicity of the DNA. Other types of polysaccharides and their modification, such as chitosan and starch, have been applied to the binder for high capacity anodes [16,17]. Such linear polysaccharides have been studied extensively, whereas research on the application of branched polysaccharides to the LIB binder is still required.

Pectin (Pec) material is the linear polysaccharide applied most recently to LIBs. Yoon et al. [18] reported that Pec composed of $\alpha$-glycosidic bonds with -COOH functional groups resulted in superior cycling ability and rate capability of silicon anodes to CMC of $\beta$-glycosidic bonds with -COOH, and amylose of $\alpha$-glycosidic bonds without -COOH. On the other hand, the modification of Pec by grafting and crosslinking has been suggested to cope with these limitations because of the low chemical resistance and poor compact ability of Pec [19]. Similar to alginate, Pec contains numerous carboxyl and hydroxyl groups on chain-chain association and easily forms a physical crosslink with divalent cations, such as $Ca^{2+}$ [20]. On the other hand, the crosslinked Pec network was more elastic than the crosslinked alginate network when they were linked with divalent calcium cations [20,21]. In practice, the elastic property might be more beneficial to high capacity anodes experiencing large volume changes during cycling. Zhu et al. [22] reported

†To whom correspondence should be addressed.
E-mail: esoh1@ulsan.ac.kr

that a highly stretchable crosslinked polyacrylamide (PAAm) had high strain resistance for the expansion of silicon electrodes as well as strong affinity to bonding with the nano-Si surface, leading to remarkable cycling performance of the silicon electrode. Recently, the dual-crosslinked binder of alginate with PAAm was reported to be effective in improving the electrochemical performance of silicon/graphite electrodes owing to the intrinsic good binding property, enhanced lithium ion transport, and extremely low volume expansion [23].

In this study, a dual-crosslinked binder of Pec with PAAm was newly constructed for high capacity silicon/graphite anodes. Pec was first grafted with PAAm, and ionic and chemical crosslinking were then performed to complete the dual-crosslinking in the grafted polymer. A variety of characterization tools were used to examine the electrochemical performance of the electrodes containing the Pec-PAAm dual-crosslinking binder system, which was compared with that of the alginate-PAAm binder system.

## EXPERIMENTAL

### 1. Synthesis of Pectin Grafted/Crosslinked with Polyacrylamide

One-step free thermal polymerization was used to produce Pec-*g*-PAAm, i.e., pectin grafted with polyacrylamide. A solution containing 2.8 g of Pec and 10 g of acrylamide monomer (AAm) in 50 ml water was placed in a three-necked flask with a mechanical stirrer for 24 h. Before a free radical initiator was added, nitrogen bubbling was performed to eliminate the oxygen in the solution for one hour because oxygen easily inhibits the free radical polymerization. Ammonium persulfate (APS, 0.06 g in 5 ml $H_2O$) as a radical initiator and tetramethyl-ethylenediamine (TEMED, 0.055 g) as a reaction accelerator were added to the mixed solution followed by heating to 50 °C. The solution was well mixed and maintained at that temperature for 3 h under nitrogen atmosphere to complete the grafting of Pec with PAAm, Pec-*g*-PAAm. The resulting viscous solution was precipitated using acetone and washed with the mixture of ethyl alcohol and water several times to remove unreacted monomers including small molecules. All chemicals used were purchased from Sigma-Aldrich Co. Ltd. More details on the grafting procedure are described in a previous study [23]. For the physical crosslinking of Pec by divalent cations, *c*-Pec, a small amount of 2 wt% $CaCl_2$ was added to a 5 wt% aqueous Pec solution and stirred for 30 min under a nitrogen atmosphere, leading to a high viscosity reaction mixture. The reaction mixture was kept overnight in a convection oven at 70 °C. The physical crosslink of Pec in the Pec-*g*-PAAm was also achieved using $CaCl_2$, and N,N′-methylenebis(acrylamide) (MBAA) was used for chemical crosslinking of PAAm chains in the Pec-*g*-PAAm. This dual-crosslinked sample is called *c*-Pec-*g*-PAAm.

### 2. Preparation of Electrodes and Cells

For slurry preparation, silicon (30-50 nm, KCC Co. Ltd.)/graphite (MAGD, D50=21 μm, Hitachi) with a weight ratio of 1/3, 5 wt% water-dispersed carbon nanotubes as a conducting agent, and 5 wt% water-based binders (Pec or Pec-*g*-PAAm) were mixed in water with a weight ratio of 76 : 9 : 15. The well-mixed slurry was cast onto copper foil using the doctor-blade method, dried in a convection oven at 70 °C for 30 min, and then dried continuously in a vacuum oven at 70 °C overnight. To crosslink the binder either physically or physically-chemically, a small amount of $CaCl_2$ or $CaCl_2$ and MBAA with APS was added to the slurry composed of silicon/graphite: conducting agent: binder at the same weight ratio of 76 : 9 : 15, and the same procedure mentioned above was performed to dry the electrodes. The mass loading of the Si/C electrodes was 1.9±0.1 mg $cm^{-2}$. CR2032 coin-half cells were assembled in an argon-filled glove-box using the Si/C working electrode, and Li foil as the counter and reference electrodes. The electrolyte was 1.15 M $LiPF_6$ in ethylene carbonate (EC) : diethyl carbonate (DEC) : dimethyl carbonate (DMC) 3 : 5 : 2 by volume with additives (5 wt% fluoroethylene, 2 wt% vinylene carbonate and 0.4 wt% $LiBF_4$) (Enchem Co. Ltd.), and polypropylene film (Celgard LLC) was used as a separator.

### 3. Physical Characterization of the Polymers

All polymeric binder samples for characterization were prepared by a solution casting method and then dried overnight in a vacuum oven at 70 °C. The Pec-based polymers were analyzed by Fourier-transform infrared (FT-IR, Thermo Scientific Nicolet iS5) spectroscopy over the range, 4,000-400 $cm^{-1}$. Thermogravimetric analysis (TGA, Q50, TA Instruments) of the polymer binders was performed in a nitrogen atmosphere. For TGA, 15 mg of the sample was placed in a platinum pan and heated from room temperature to 600 °C at 10 °C $min^{-1}$. The electrolyte uptake of the binder was measured by immersing the dried polymer film into 20 ml of mixed carbonates, a mixture of ethylene carbonate (EC) : diethylcarbonate (DEC) : dimethyl carbonate (DMC) at 1 : 1 : 1 vol%. The films were taken out after 48 h and wiped to remove the excess carbonate adsorbed on the surface. The swelling ratio was calculated from the difference in the weight of the films before and after electrolyte soaking.

The binder films were elongated at room temperature using a texture analyzer (TA-PLUS, Lloyd Instruments Ltd.). To prepare the test samples, grafted copolymer was first dissolved in distilled water at room temperature, and 30 wt% glycerol to polymer as a plasticizer was added to the solution. After stirring for 15 min, the physical and chemical agents were added to the mixture followed by 10 min stirring. The solution was then poured into a petri dish and dried overnight in a convection oven at 50 °C. Subsequently, the film was cut into strips (10×50 cm) and mounted between the abrasive papers. The tension speed of the film strips was 5 mm $min^{-1}$.

### 4. Physical and Electrochemical Characterizations of Electrodes

Using a texture analyzer, the adhesion strength of the Si/C electrode was obtained by measuring the 180° peeling force of the electrode strips with a peeling speed of 20 mm $min^{-1}$. For a more realistic situation, all the samples were soaked in carbonate electrolyte medium for one day, immersed into DMC solvent to remove the surface electrolyte, and finally dried at room temperature for 20 min before being peeled. A video-connected device (Theta Lite 100, KSV Instrument Ltd.) was used to measure the contact angles of the Si/C electrodes. The galvanostatic charge/discharge of the coin-half cells was performed between 5 mV and 1.5 V at a current rate of 0.1 C for the first two cycles and at 0.5 C for the following 100 cycles. Electrochemical impedance spectroscopy (EIS) over the frequency range, 100 kHz to 0.01 Hz, and cyclic voltammetry (CV) of the coin-half cells were performed using a BioLogic Science

Instrument.

## RESULTS AND DISCUSSION

### 1. Polymeric Binder Characterization

The dual-crosslink between Pec and PAAm was performed in an aqueous medium using a two-step method. First, the Pec-*g*-PAAm binder was synthesized by grafting PAAm onto Pec using a redox initiator system, APS/TEMED, and then the graft copolymer was linked with a physical crosslinker ($CaCl_2$) and chemical crosslinker (MBAA). Coordinate bonds of the hydroxyl and carboxyl groups with $Ca^{2+}$ ions were formed in the main chain of Pec and the PAAm side chains in the graft copolymer were bonded covalently with MBAA. Fig. S1 presents the synthesis scheme with the chemical structures, including the dual-crosslinked *c*-Pec-*g*-PAAm.

Successful formation of the Pec-*g*-PAAm polymer was first confirmed by FT-IR spectroscopy, as shown in Fig. 1(a). The FT-IR spectrum of Pec showed several peaks: a broad peak at 3,410 $cm^{-1}$ for the -OH group, a peak at 2,940 $cm^{-1}$ for the -$CH_2$ group of alkane, two sharp peaks at 1,748 and 1,632 $cm^{-1}$ for -COOH groups, and a peak at 1,444 $cm^{-1}$ for the -$CH_2$ of the secondary alcohol. The stretching vibration of C-O as complex bands, which resulted from an ether (C-O-C) and cyclic alcohol (CH-OH) in the saccharide chain, was also observed at 1,000 to 1,300 $cm^{-1}$: two peaks at 1,266 and 1,102 $cm^{-1}$ for the C-O stretching band in the cyclic alcohol, and two peaks at 1,147 and 1,014 $cm^{-1}$ for the C-O stretching vibration in the ether [19]. Owing to the formation of ether bonds between the hydroxyl group placed in anhydroglucose C2 and the p band of PAAm, the adsorption peaks at 1,266 $cm^{-1}$ (C-O stretching) and 632 $cm^{-1}$ (C-OH bending) were almost absent in the spectrum of Pec-*g*-PAAm. In contrast, the overlapped peaks attributed to the ether and cyclic alcohol still remained in the range, 1,150 to 1,000 $cm^{-1}$, but their intensities were lower. On the other hand, the adsorption peaks related to PAAm [24], the anti-symmetric and symmetric stretching vibrations of $NH_2$ at 3,480 and 3,180 $cm^{-1}$, an overlapped band from C=O stretching vibration and $NH_2$ deformation band around 1,651 $cm^{-1}$, and the C-N stretching band at 1,413 $cm^{-1}$, were observed in the FT-IR spectrum of Pec-*g*-PAAm, but all peaks were shifted compared to the original PAAm spectrum. This suggests that a graft reaction between Pec and AAm monomers had occurred. Fig. 1(a) presents the FT-IR spectrum of *c*-Pec-*g*-PAAm. The adsorption bands of the graft Pec-*g*-PAAm copolymer at 3,480 $cm^{-1}$ (-OH) and 1,651 $cm^{-1}$ (asymmetric COO-) were shifted in the dual-crosslinked *c*-Pec-*g*-PAAm. This was attributed to the strong coordination bonds between $Ca^{2+}$ ions and Pec in the graft copolymer [13,14]. In the next, the spectrum of *c*-Pec-*g*-PAAm showed sharp peaks at 1,452, 1,112, and 603 $cm^{-1}$, which were associated with N-H bending, C-N stretching, and N-C=O bending in the amide groups of the chemical crosslinker

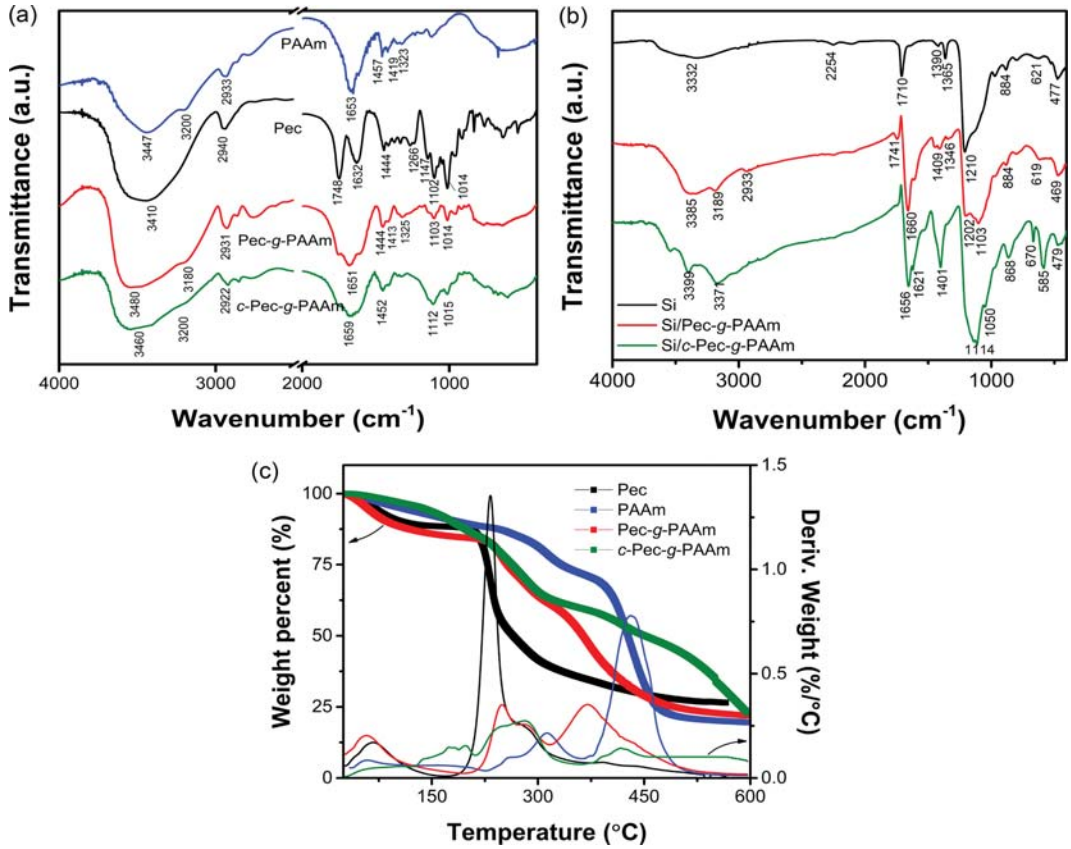


**Fig. 1. (a) FT-IR spectra of as-synthesized PAAm, natural Pec, Pec grafted with PAAm (Pec-g-PAAm), and dual-crosslinked c-Pec-g-PAAm, (b) FT-IR spectra of pure Si, slurry of Si and Pec-g-PAAm, and slurry of Si and c-Pec-g-PAAm, and (c) Thermal gravimetric analysis of the binders.**

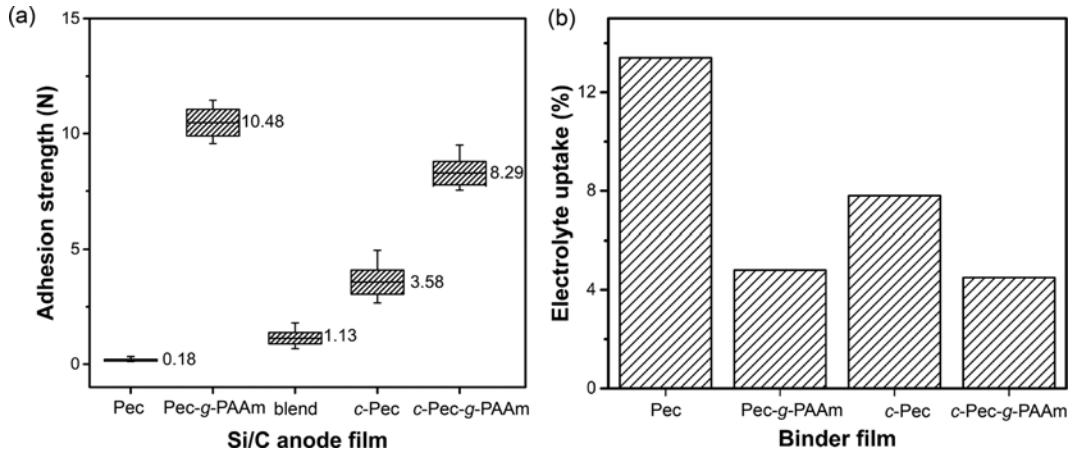


**Fig. 2. (a) Adhesion strength of Si/C electrodes containing different binders measured using the 180° peel test, and (b) electrolyte uptake of polymer films immersed in the electrolyte solvent (EC : DMC : EMC) at 25 °C for 48 h.**

MBAA, respectively [24]. This was attributed to the presence of additional amide groups in MBAA as well as the amides in the graft polymer.

To confirm the formation of dual-crosslinked network of the binder in the presence of Si active materials, silicon active materials were added to an appropriate amount of Pec-*g*-PAAm solution and mixed with or without the crosslinking agents. As shown in Fig. S2, the slurry sample with the crosslinkers formed a gel-like phase, indicating the possibility of crosslinking. This was also clarified from a comparison of the FT-IR spectra of the slurry samples (Fig. 1(b)). As mentioned above, the peak at 1,656 $cm^{-1}$ in the spectrum of the Si/*c*-Pec-*g*-PAAm sample indicated the formation of the ionic crosslinking between the carboxyl groups and $Ca^{2+}$. In addition, the peak at 1,741 $cm^{-1}$ attributed to C=O stretching in the carboxylic acid was weakened by limiting the stretching due to ionic crosslinking. The sharp peaks at 1,401 and 585 $cm^{-1}$ were assigned to C-N stretching and N-C=O bending bands of the secondary amide in the chemical crosslinker, MBAA [25]. On the other hand, the strong peaks at 1,114 and 868 $cm^{-1}$ were assigned to an ester-like bond between the binder and Si particles, which is a strong covalent bond produced from a reaction between the carboxyl groups in the binder and silanol groups (Si-OH) at the surface of the Si particles [26,27]. Overall, the grafted Pec-*g*-PAAm and its dual-crosslinked *c*-Pec-*g*-PAAm had been successfully synthesized.

TGA of the polymers was also performed and the result is presented in Fig. 1(c). The main thermal degradation of pure Pec, corresponding to a weight loss of 48.8%, occurred over the temperature range of 200-320 °C. As-synthesized PAAm has two thermal degradation steps with the exception of the low temperature weight loss below 150 °C caused by water evaporation. From 230 to 340 °C, 14.1% weight loss was observed, which was attributed to the degradation of amino groups [28]. A major weight loss of 50.2% was noted in the range of 380-520 °C, attributed to decomposition of the backbone chain to carbon dioxide and hydrocarbons. For Pec-*g*-PAAm, the thermal stability was characterized as improved compared to pure Pec but no better than pure PAAm. Two thermal decomposition peaks related to Pec chains and acrylamide chains were observed between 220-310 °C with a weight loss of 21.4%. The third decomposition occurred over a relatively broad temperature range between 320 °C and 520 °C with a large weight loss of 37.0% due to decomposition of the polymer backbone. In contrast, the dual-crosslinked *c*-Pec-*g*-PAAm sample was resistive to the high temperature decomposition of the polymer backbone above 320 °C. This suggests that the chemical crosslinking caused by MBAA also helps improve the thermal resistance of the PAAm backbone chain.

**2. Slurry Characterization**

An increase in the interaction between polymeric binders and hydroxyl groups on the Si surface through hydrogen or covalent bonds leads to an improvement in the adhesion of the Si-based anode [29,30]. The adhesion capability of the binder in the Si/C electrodes was estimated using a 180° peel test, as illustrated in Fig. 2(a). All modified Pec samples with grafting and/or crosslinking showed significantly higher adhesion than natural Pec. In particular, the grafted copolymers showed much higher adhesion than the physical blend between Pec and PAAm. This was attributed to the multipoint functional groups in the grafted structure for Pec-*g*-PAAm, which form a more flocculated structure with strong hydrogen bonds in the electrode [12]. On the other hand, the dual-crosslinking by $Ca^{2+}$ and MBAA increases the interconnection among the polymer chains in the Pec-*g*-PAAm. This decreases the number of functional groups of the binder, which are normally connected to the active materials. This may explain the slight decrease in the 180° peel strength of the dual-crosslinked *c*-Pec-*g*-PAAm (8.29 N load force), compared to the grafted Pec-*g*-PAAm binder (10.48 N load force).

The adhesion sustainability of the polymeric binder in the electrode is affected by the amount of solvent uptake causing swelling of the binder, ultimately leading to a weakened interaction between the active materials and current collector [30,31]. Fig. 2(b) presents the electrolyte uptake of all binder samples. Pec showed an approximately 13% electrolyte uptake, which is relatively larger than that of the other modified Pec samples. The poor adhesion of the Pec binder in Fig. 2(a) may be due partially to the large electrolyte uptake. A previous study [23] reported that PAAm was quite

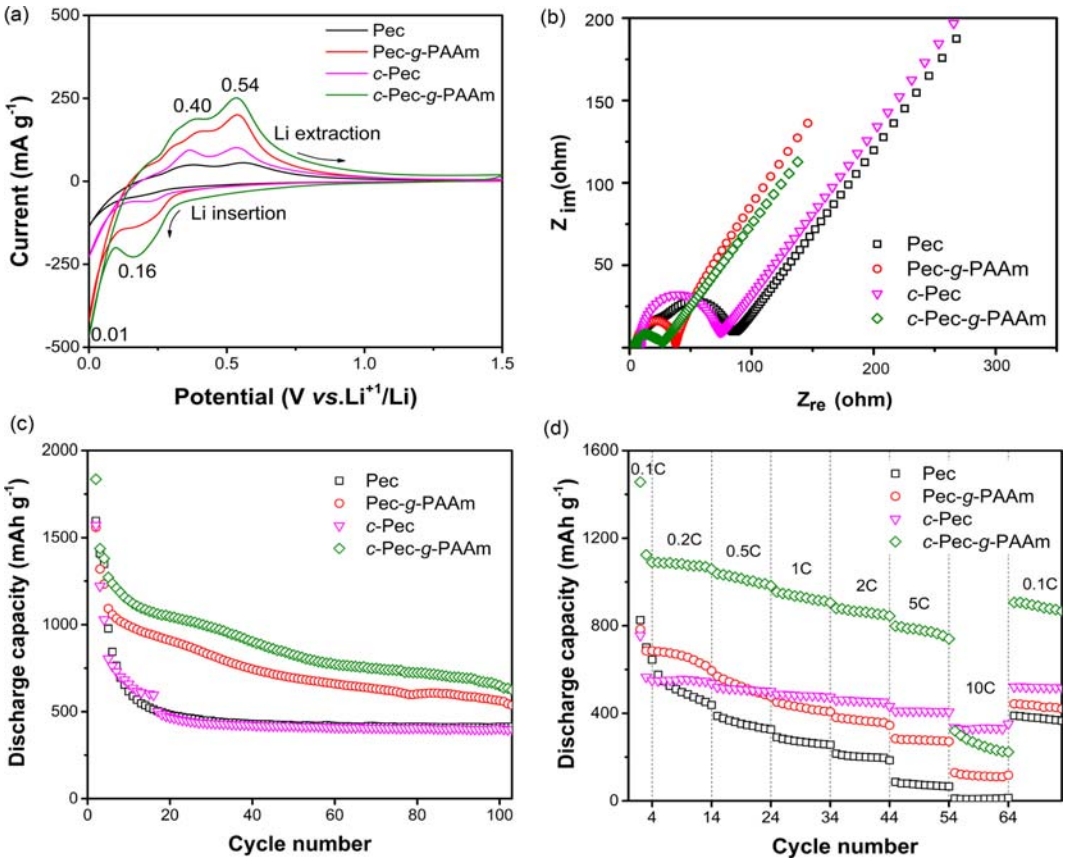


**Fig. 3. (a) Cyclic voltammogram of the fresh Si/C electrodes containing different binders, (b) EIS of the Si/C electrodes measured at 0.2 V, (c) cyclic performance, and (d) rate capacity test of the Si/C electrodes.**

resistant to carbonate electrolyte swelling with an uptake of less than 2%, even though it will be shown later that PAAm has affinity to carbonate due to the presence of carbonyl dipoles in the amide groups. Therefore, the modified Pec samples containing PAAm have much lower electrolyte uptake, which helps maintain the integrity of the Si/C electrodes during long-term cycling.

### 3. Electrochemical Characterizations

The effects of modifying the Pec binder on the electrochemical properties of Si/C anodes were investigated by CV, EIS, and galvanostatic cycle tests. Fig. 3(a) shows the CV profiles of the Si/C fresh electrodes obtained in the voltage range of 0 to 1.5 V (*vs.* $Li^+/Li$) with a scan rate of 0.2 mV $s^{-1}$. All fresh electrodes displayed two pairs of redox peaks: two cathodic peaks at approximately 0.0 and 0.2 V for Li insertion and two anodic peaks at approximately 0.4 and 0.5 V for Li extraction. The Si/C electrodes containing the PAAm modified-Pec binders exhibited higher redox currents than that containing the natural Pec binder. This might be due to the superior electrolyte wettability of the PAAm modified-Pec to the Pec binder. The strong carbonyl dipole (C=O) in an amide must have an affinity for the carbonyl groups in the carbonate structure so that the Si/C electrodes containing the PAAm form considerably low contact angles with the electrolyte, as shown in Fig. S3. This indicates rapid penetration of electrolyte into the electrode, which leads to a broader available active area for the CV experiment. Thus, the PAAm-containing binder helps provide good contact of the electrode particles to the carbonate electrolyte, resulting in more lithium ion movement through the electrode. In particular, the significant increase in the redox CV peaks of the Si/C electrode with the *c*-Pec-*g*-PAAm binder could be attributed to the effective integration of the electrode and an improvement in ion transport caused by dual-crosslinking.

This was confirmed by EIS, as shown in Fig. 3(b). EIS of the Si/C electrodes was performed at 0.2 V after two precycling steps at 0.1 C followed by two more cycles at 0.5 C. The semicircle at the middle frequency range indicated the charge transfer resistance of the electrochemical reaction occurring at the interface, which is closely related to the ion and electron transport characteristics. PAAm-containing binders, in particular, the dual crosslinked *c*-Pec-*g*-PAAm binder, lead to the lowest charge transfer resistance. In addition, the low frequency Warburg region of the EIS enables a calculation of the diffusion coefficients of lithium ions using the following equation:

$$D = 0.5\left(\frac{RT}{AF^2\sigma_\omega C}\right)^2 \quad (1)$$

where A, F, C, R, and T are the surface area, Faraday constant, concentration of lithium ions in the solid, gas constant, and temperature, respectively [32]. $\sigma_\omega$ indicates the slope of the real part of the impedance versus $\omega^{-0.5}$ (angular frequency in the Warburg region). Based on the slope shown in Fig. S4, the diffusion coefficients cal-

culated using the above equation were $5.0\times10^{-12}$, $3.5\times10^{-12}$, $17.7\times10^{-10}$, and $14.0\times10^{-10}$ $cm^2$ $s^{-1}$ for the Pec, *c*-Pec, Pec-*g*-PAAm, and *c*-Pec-*g*-PAAm electrodes, respectively. In summary, the dual-crosslinked binder improves the charge transfer kinetics and mass transport in the electrode compared to the other binders.

From the cyclic performance test shown in Fig. 3(c), the Si/C electrodes with Pec and *c*-Pec experienced a severe drop in discharge capacity to below 500 mAh $g^{-1}$ during the first 20 cycles, followed by stable capacity of approximately 415 mAh $g^{-1}$. This initial severe drop must be responsible for the weak binding strength to endure huge volume change in the Si component, as shown in Fig. 2(a). On the other hand, the reversible capacity of the Si/C electrode remained around 540 mAh $g^{-1}$ at 100 cycles when the Pec binder was grafted with PAAm with a much slower decay in the capacity for the first tens of cycles. The target Si/C electrode construct with dual crosslinking in the binder, *c*-Pec-*g*-PAAm, provided further improvement in the cycling capacity; it was 625 mAh $g^{-1}$ at the 100$^{th}$ cycle. A comparison of the average discharge capacities within 100 cycles revealed the *c*-Pec-*g*-PAAm-containing electrode to have the highest value of 861 mAh $g^{-1}$, followed in order by 732, 463, and 451 mAh $g^{-1}$ for Pec-*g*-PAAm, Pec, and *c*-Pec, respectively. Grafting with PAAm helps improve the mechanical stability of the electrode due to the numerous multipoint functional groups [23], as observed from the strong adhesion of Pec-*g*-PAAm (Fig. 2(a)). The chemical crosslinking in PAAm and physical crosslinking in Pec improved the robustness of the network against significant strain in the Si/C electrode [22,23]. On the other hand, a decrease in the Si/C mass loading from 1.9 to 0.9 mg $cm^{-2}$ greatly increased the capacity retention, as calculated by the ratio of the capacity at the 100$^{th}$ cycle to that at the second cycle, from 45% to 68% (Fig. S5). The average discharge capacity within 100 cycles was 868 mAh $g^{-1}$, which is much larger than that with a 1.9 mg $cm^{-2}$ mass loading.

The effects of the binder on the rate capability of the Si/C electrodes were also examined through various current densities in the range, 0.1 C to 10 C, as shown in Fig. 3(d). The Si/C electrode containing the dual crosslinked *c*-Pec-*g*-PAAm binder exhibited overwhelmingly superior rate performance to the other electrodes except at the highest current density, 10 C. The Si/C with *c*-Pec-*g*-PAAm retained 79.9% capacity at a 0.2 C current at a 5 C rate and maintained more than 786 mAh $g^{-1}$, whereas the capacities of the other electrodes were less than 425 mAh $g^{-1}$ at 5 C and their capacity retention at 5 C over 0.2 C were 16.7%, 43.2%, and 74.8% for Pec, Pec-*g*-PAAm, and *c*-Pec, respectively. Although the dual-crosslinked Si/C had an unexpectedly low capacity of 311.3 mAh $g^{-1}$ at the highest current density of 10 C, the capacity was restored rapidly to 822.4 mAh $g^{-1}$ when the current was returned to 0.1 C.

The surface morphology of 100-cycled Si/C electrodes was characterized by plan view field-emission scanning electron microscopy (FE-SEM Jeol, JSM-6500F) to determine the mechanical stability of the electrode film. As shown in Fig. 4, all electrodes except for the dual-crosslinked electrode exhibited distinct cracks caused by severe volume changes. The Si/C electrode containing the *c*-Pec-*g*-PAAm binder showed no obvious cracks and the dual-crosslinking network formed by the binder plays an important role in the long-term cycling stability. This can be supported by the change in electrode thickness between the fresh and 10-cycled electrodes, as shown in Fig. S6. The changes in thickness of the Si/C electrode after 10 cycles were 55.8 μm (131%) from 42.6 μm for the Pec-containing electrode, 53.8 μm (124%) from 43.3 μm for the *c*-Pec-containing electrode, 35.8 μm (84%) from 42.6 μm for the Pec-*g*-PAAm-containing electrode, and 32.8 μm (74%) from

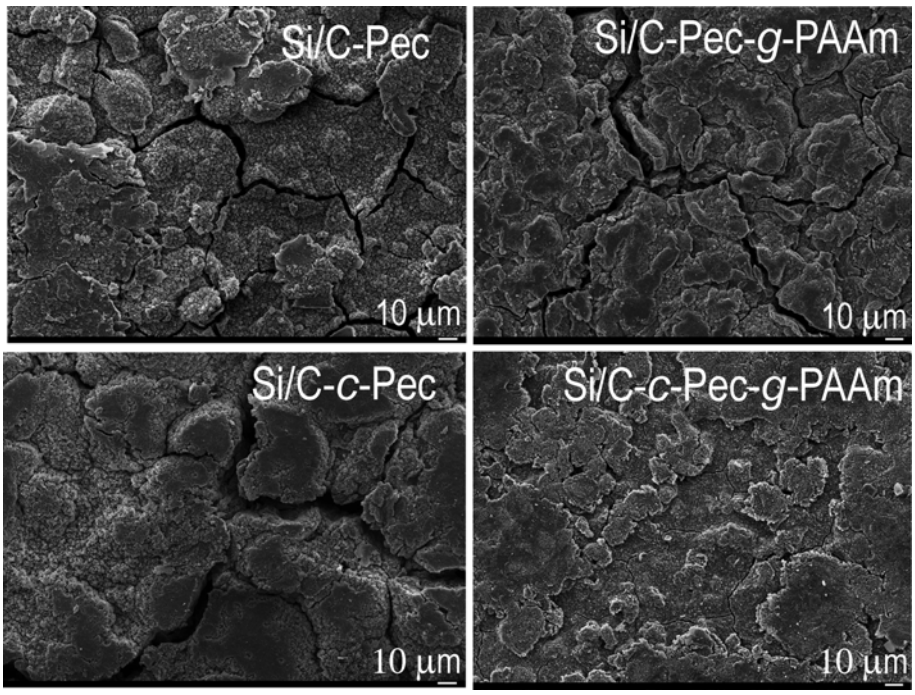


**Fig. 4. Top-view SEM-images of the Si/C electrodes after 100 cycles.**

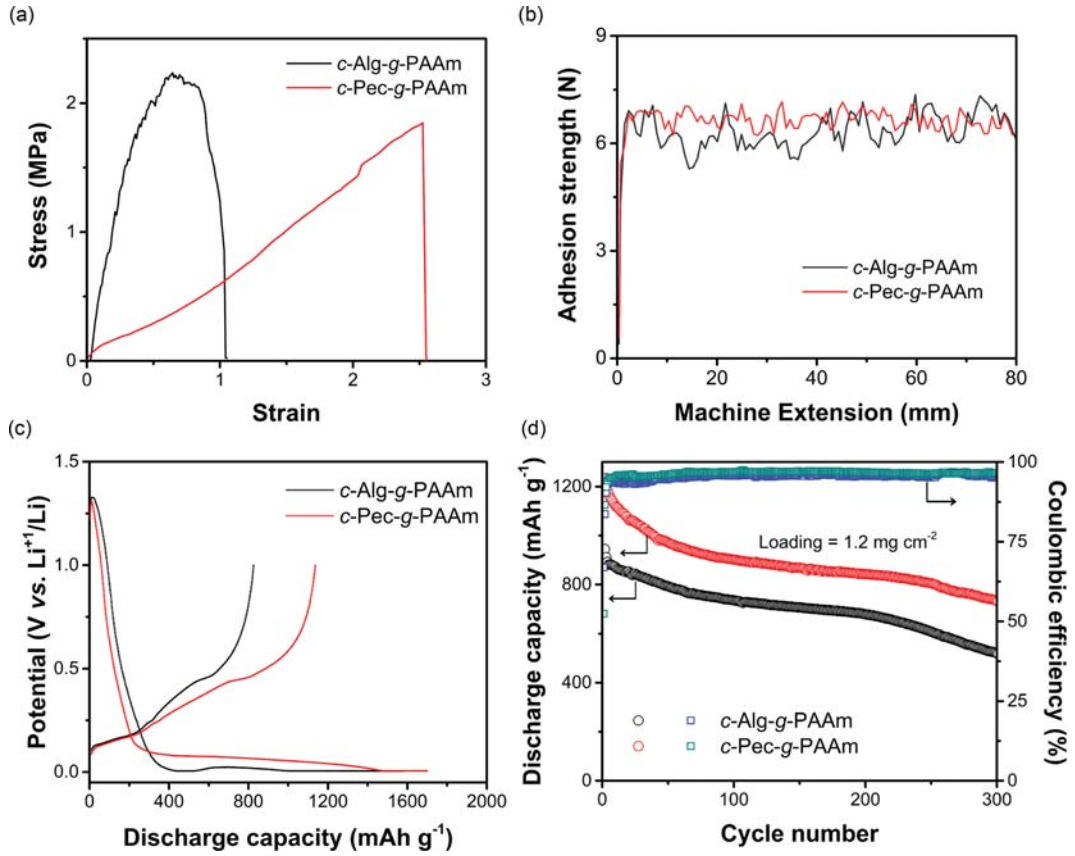


**Fig. 5. (a) Elongation at break of Alg and Pec-based dual-crosslinked binder films, (b) adhesion strength measured according to 180° peel strength, (c) initial charge/discharge profiles, and (d) cyclic performance of the Si/C electrodes with c-Alg-g-PAAm and *c*-Pec-*g*-PAAm.**

44.4 μm for the *c*-Pec-*g*-PAAm electrode. Therefore, the strong dual-crosslinking network is effective in reducing the extra volume expansion during the cycle and may help improve the cycling ability and rate-capacity retention of the Si/C electrode containing *c*-Pec-*g*-PAAm.

The crosslinked Pec network, *c*-Pec, is more elastic than crosslinked alginate, *c*-Alg, in biochemical applications when they are crosslinked physically with $Ca^{2+}$ [21]. Therefore, it is important to compare the dual-crosslinked *c*-Pec-*g*-PAAm with the dual-crosslinked *c*-Alg-*g*-PAAm as a binder for the Si/C anode. A previous study [23] reported that *c*-Alg-*g*-PAAm was an effective binder for Si/C electrodes. Herein, a comparative study of the cyclic performance of high capacity Si/C electrodes was conducted using alginate and Pec-based dual-crosslinked binders, as shown in Fig. 5. The elongation characterization of the dual-crosslinked polymeric film containing 30 wt% glycerol plasticizer suggests that *c*-Alg-*g*-PAAm is more brittle with higher stress and lower strain at break than *c*-Pec-*g*-PAAm. Silva et al. [20] also reported that the tensile strength of alginate-based samples was randomly higher with a low elongation than Pec and its composite film. This was attributed to the difference in ionic crosslinking. Pectin forms a flexible dot-ionic crosslinking in the presence of $Ca^{2+}$, whereas alginate forms a semi-flexible network by a zip-ionic crosslink with the divalent ions [21,33]. Before comparing their electrochemical performance, the 74% volume expansion of the Si/C-*c*-Pec-*g*-PAAm electrode shown in Fig. S6 was relatively larger than the 4% expansion of the Si/C-*c*-Alg-*g*-PAAm electrode (Fig. 7 in [23]). This was attributed to the difference in their elastic moduli.

The Si/C anode with *c*-Pec-*g*-PAAm showed slightly higher adhesion ability with an average value of 6.59 N in the 180° peel strength of the anode film, as shown in Fig. 5(b). With the same loading of 1.2 mg $cm^{-2}$, the *c*-Pec-*g*-PAAm-containing Si/C electrode exhibited higher reversible capacity under cycling at 0.1 than the *c*-Alg-*g*-PAAm-containing electrode. Furthermore, as shown in Fig. 5(d), the cycle performance test cycled up to 300 cycles at 0.5 C revealed the *c*-Pec-*g*-PAAm binder to produce superior cyclic capacity over the *c*-Alg-*g*-PAAm binder. The Si/C-*c*-Pec-*g*-PAAm electrode retained 729 mAh $g^{-1}$ (59% capacity retention) after 300 cycles, whereas the Si/C-*c*-Alg-*g*-PAAm electrode retained only 516 mAh $g^{-1}$ (57% capacity retention). Consequently, Pec can form a more favorable dual-crosslinked network in a high capacity anode than alginate.

## CONCLUSIONS

The modification of a polysaccharide polymer, pectin, through grafting and crosslinking with polyacrylamide was quite effective as an adhesive water-soluble binder in high capacity silicon anodes to endure the huge volume changes of Si/graphite composite electrodes. The pectin grafted with polyacrylamide, Pec-*g*-PAAm, poly-

meric binder was synthesized by an in-situ polymerization method using a redox initiator in an aqueous medium. The dual-crosslinked polymer, *c*-Pec-*g*-PAAm, was prepared from the graft copolymer in the presence of two crosslinking agents, $CaCl_2$, as an ionic crosslinker, and MBAA, as a chemical crosslinker, during the preparation process of the electrode slurry. The PAAm in the graft copolymer improved the mechanical strength of the electrodes through strong adhesion and facilitated electrolyte-penetration with low electrolyte swelling, leading to good mechanical stability and lithium ion movement through the Si/C electrode. Moreover, the dual-crosslinking in the target binder contributed to the efficient integration of the electrode and a further decrease in polarization resistance. As a result, the dual-crosslinking network prevents severe volume expansion of the high capacity Si/C electrode during the cycling and maintains good cycling ability and rate-capacity retention. Compared to the dual-crosslinked alginate with PAAm (*c*-Alg-*g*-PAAm), *c*-Pec-*g*-PAAm forms a more flexible network and is more beneficial to the cycling performance of high capacity anodes.

Consequently, pectin polysaccharide is also a good choice to form a dual-crosslinked network with PAAm in high capacity anodes, ultimately resulting in long-term stability with high capacity.

## ACKNOWLEDGEMENTS

The study was supported by the 2018 research fund of the University of Ulsan.

## SUPPORTING INFORMATION

Additional information as noted in the text. This information is available via the Internet at http://www.springer.com/chemistry/journal/11814.

## REFERENCES

1. A. S. Aricò, P. Bruce, B. Scrosati, J.-M. Tarascon and W. van Schalkwijk, *Nat. Mater.*, **4**, 366 (2005).
2. M. Armand and J.-M. Tarascon, *Nature*, **451**, 652 (2008).
3. B. Li, Y. Wang and S. Yang, *Adv. Energy Mater.*, **8**, 1702296 (2018).
4. H. Buqa, M. Holzapfel, F. Krumeich, C. Veit and P. Novák, *J. Power Sources*, **161**, 617 (2006).
5. W.-R. Liu, M.-H. Yang, H.-C. Wu, S. M. Chiao and N.-L. Wu, *Electrochem. Solid-State Lett.*, **8**, A100 (2005).
6. A. Magasinski, B. Zdyrko, I. Kovalenko, B. Hertzberg, R. Burtovyy, C. F. Huebner, T. F. Fuller, I. Luzinov and G. Yushin, *ACS Appl. Mater. Interfaces*, **2**, 3004 (2010).
7. H.-K. Park, B.-S. Kong and E.-S. Oh, *Electrochem. Commun.*, **13**, 1051 (2011).
8. J. Li, R. B. Lewis and J. R. Dahn, *Electrochem. Solid-State Lett.*, **10**, A17 (2007).
9. I. Kovalenko, B. Zdyrko, A. Magasinski, B. Hertzberg, Z. Milicev, R. Burtovyy, I. Luzinov and G. Yushin, *Science*, **334**, 75 (2011).
10. N. Lin, Y. Han, L. Wang, J. Zhou, J. Zhou, Y. Zhu and Y. Qian, *Angew. Chem. Int. Ed.*, **54**, 3822 (2015).
11. Z. Yi, W. Wang, Y. Qian, X. Liu, N. Lin and Y. Qian, *ACS Sustainable Chem. Eng.*, **6**, 14230 (2018).
12. L. Wei, C. Chen, Z. Hou and H. Wei, *Scientific Reports*, **6**, 19583 (2016).
13. L. Zhang, L. Zhang, L. Chai, P. Xue, W. Hao and H. Zheng, *J. Mater. Chem. A*, **2**, 19036 (2014).
14. J. Liu, Q. Zhang, Z.-Y. Wu, J.-H. Wu, J.-T. Li, L. Huang and S.-G. Sun, *Chem. Commun.*, **50**, 6386 (2014).
15. S. Kim, Y. K. Jeong, Y. Wang, H. Lee and J. W. Choi, *Adv. Mater.*, **30**, 1707594 (2018).
16. C. Chen, S. H. Lee, M. Cho, J. Kim and Y. Lee, *ACS Appl. Mater. Interfaces*, **8**, 2658 (2016).
17. Y. Bie, J. Yang, Y. Nuli and J. Wang, *RSC Adv.*, **6**, 97084 (2016).
18. D.-E. Yoon, C. Hwang, N.-R. Kang, U. Lee, D. Ahn, J.-Y. Kim and H.-K. Song, *ACS Appl. Mater. Interfaces*, **8**, 4042 (2016).
19. G. S. Chauhan, A. Kumari and R. Sharma, *J. Appl. Polym. Sci.*, **106**, 2158 (2007).
20. M. A. da Silva, A. C. K. Bierhalz and T. G. Kieckbusch, *Carbohydr. Polym.*, **77**, 736 (2009).
21. Y. Fang, S. Al-Assaf, G. O. Phillips, K. Nishinari, T. Funami and P. A. Williams, *Carbohydr. Polym.*, **72**, 334 (2008).
22. X. Zhu, F. Zhang, L. Zhang, L. Zhang, Y. Song, T. Jiang, S. Sayed, C. Lu, X. Wang, J. Sun and Z. Liu, *Adv. Funct. Mater.*, **28**, 1705015 (2018).
23. B. Gendensuren and E.-S. Oh, *J. Power Sources*, **384**, 379 (2018).
24. J.-Y. Sun, X. Zhao, W. R. K. Illeperuma, O. Chaudhuri, K. H. Oh, D. J. Mooney, J. J. Vlassak and Z. Suo, *Nature*, **489**, 133 (2012).
25. L. Luo, Y. Xu, H. Zhang, X. Han, H. Dong, X. Xu, C. Chen, Y. Zhang and J. Lin, *ACS Appl. Mater. Interfaces*, **8**, 8154 (2016).
26. N. S. Hochgatterer, M. R. Schweiger, S. Koller, P. R. Raimann, T. Wöhrle, C. Wurm and M. Winter, *Electrochem. Solid-State Lett.*, **11**, A76 (2008).
27. J.-S. Bridel, T. Azaïs, M. Morcrette, J.-M. Tarascon and D. Larcher, *Chem. Mater.*, **22**, 1229 (2010).
28. D. R. Biswal and R. P. Singh, *Carbohydr. Polym.*, **57**, 379 (2004).
29. M.-H. Ryou, J. Kim, I. Lee, S. Kim, Y. K. Jeong, S. Hong, J. H. Ryu, T.-S. Kim, J.-K. Park, H. Lee and J. W. Choi, *Adv. Mater.*, **25**, 1571 (2013).
30. M. H. T. Nguyen and E.-S. Oh, *Electrochem. Commun.*, **35**, 45 (2013).
31. B.-R. Lee, S.-j. Kim and E.-S. Oh, *J. Electrochem. Soc.*, **161**, A2128 (2014).
32. N. Takami, A. Satoh, M. Hara and T. Ohsaki, *J. Electrochem. Soc.*, **142**, 371 (1995).
33. B. Zhang, B. Hu, M. Nakauma, T. Funami, K. Nishinari, K. I. Draget, G. O. Phillips and Y. Fang, *Food Res. Int.*, **116**, 232 (2019).

# Supporting Information

# Preparation of pectin-based dual-crosslinked network as a binder for high performance Si/C anode for LIBs

**Bolormaa Gendensuren, Chengxiang He, and Eun-Suok Oh†**

School of Chemical Engineering, University of Ulsan, 93 Daehak-ro, Nam-gu, Ulsan 44610, Korea
(*Received 16 September 2019 • accepted 21 November 2019*)

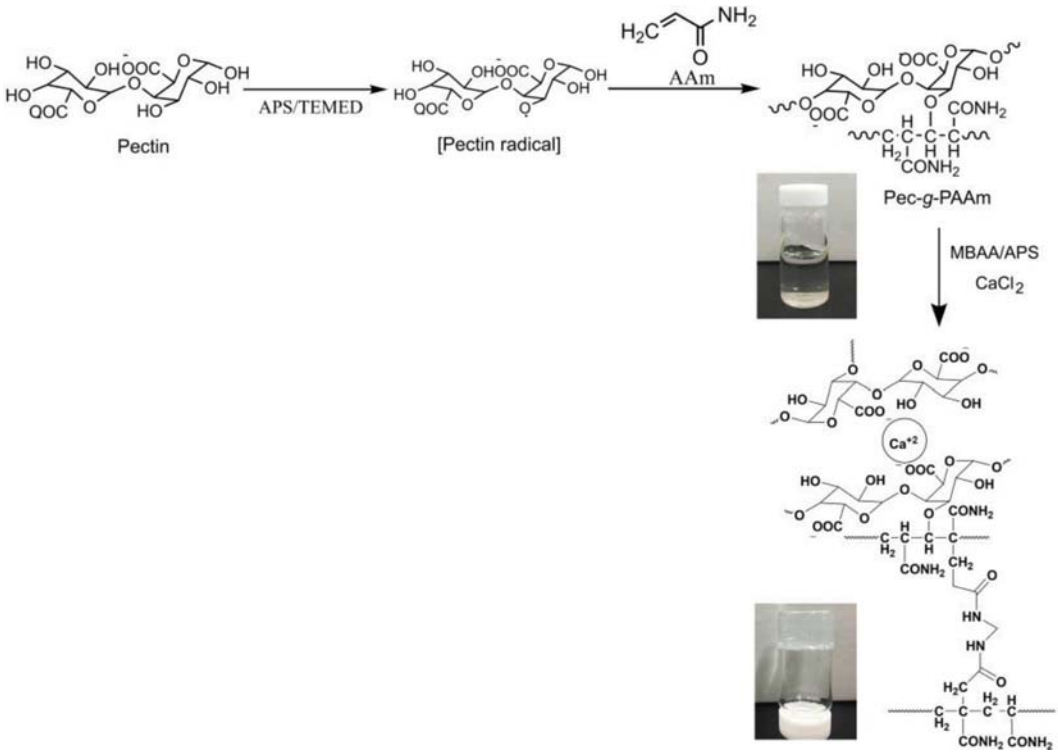


**Fig. S1. Schematic diagram of preparation of dual-crosslinked *c*-Pec-*g*-PAAm.**

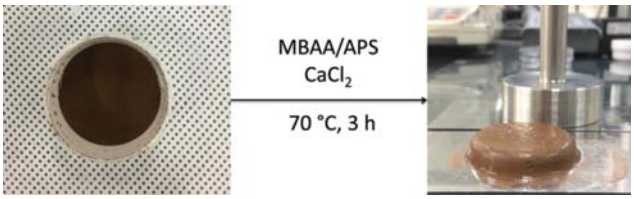


**Fig . S2. Preparation of Si slurry with the dual-crosslinked binder.**

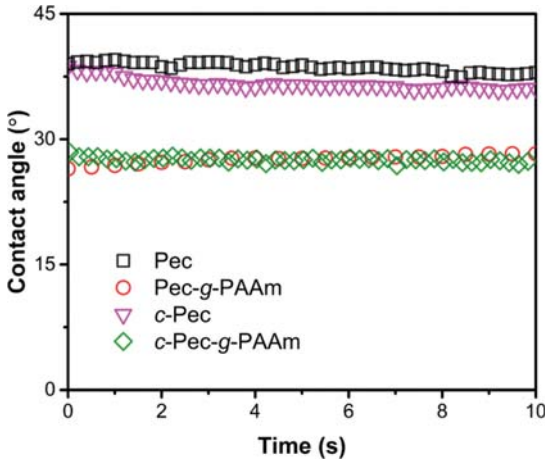


**Fig. S3. Contact angle of the Si/C electrodes with electrolyte.**

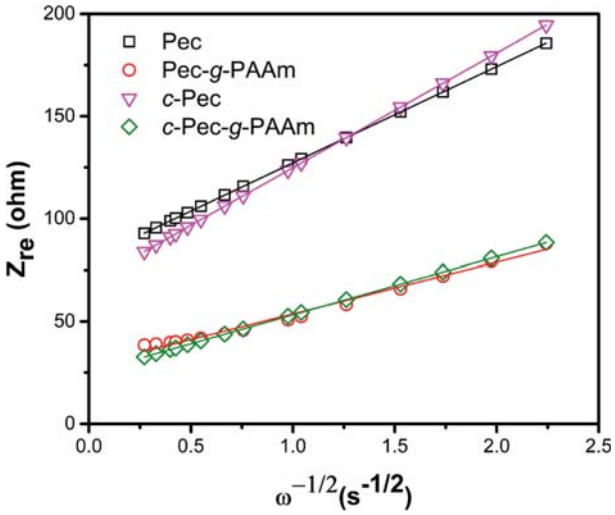


Fig. S4. Linear relationship between the real part of the impedance and the inverse square root of angular frequency in the Warburg region.

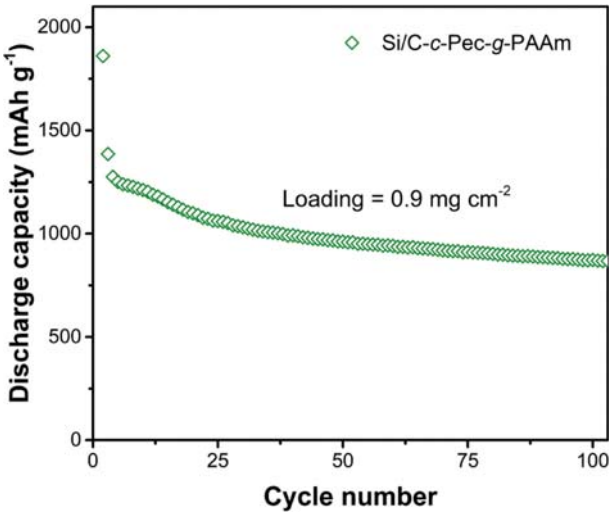


Fig. S5. Cyclic performance of the Si/C electrode containing *c*-Pec-*g*-PAAm binder at 0.5 C. The mass loading of the active material is 0.9 mg $cm^{-2}$.

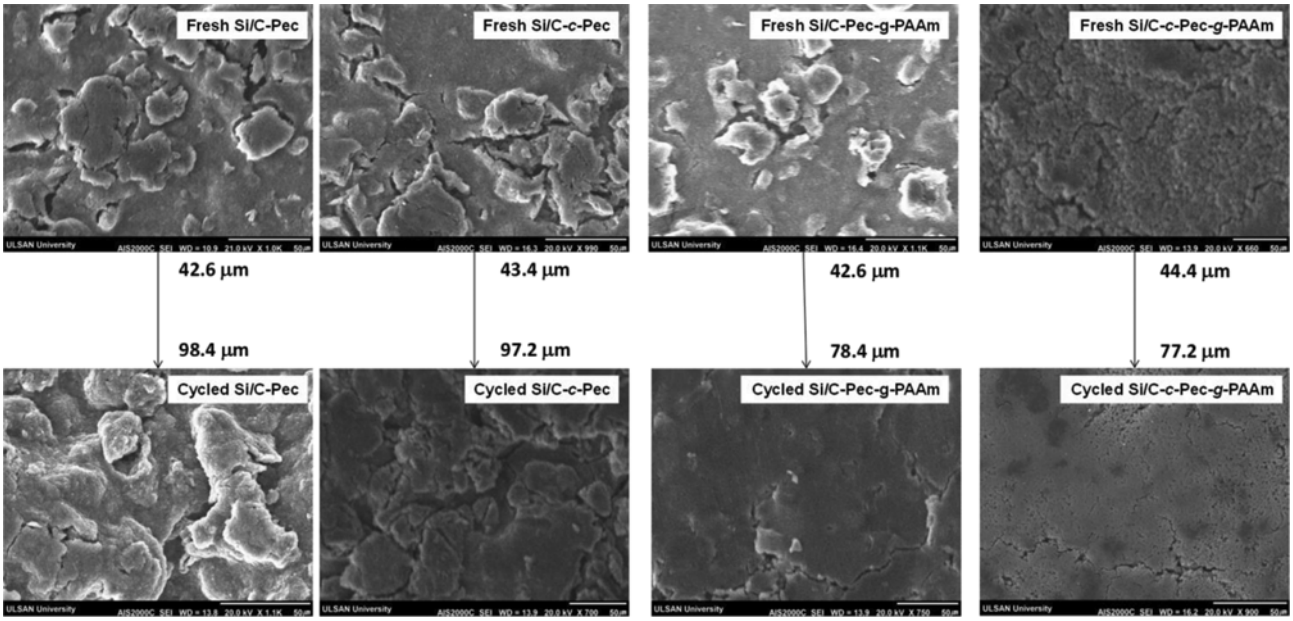


Fig. S6. Top-SEM images of Si/C electrode with four binders before and after 10 cycles. After the 10-cycled electrodes were carefully dissembled, cleaned, and dried, their thicknesses were measured using a height gauge (TESA $\mu$-HITE, Hexagon Manufacturing Intelli).